Original Article

MOLECULAR METABOLISM

Glucose-6-phosphate dehydrogenase contributes to the regulation of glucose uptake in skeletal muscle

Robert S. Lee-Young [1,*], Nolan J. Hoffman [4,9], Kate T. Murphy [5], Darren C. Henstridge [1], Dorit Samocha-Bonet [4], Andrew L. Siebel [3,10], Peter Iliades [1], Borivoj Zivanovic [1], Yet H. Hong [6], Timothy D. Colgan [2], Michael J. Kraakman [1], Clinton R. Bruce [7], Paul Gregorevic [2], Glenn K. McConell [6], Gordon S. Lynch [5], Grant R. Drummond [8], Bronwyn A. Kingwell [3], Jerry R. Greenfield [4], Mark A. Febbraio [1,4,]**

ABSTRACT

Objective: The development of skeletal muscle insulin resistance is an early physiological defect, yet the intracellular mechanisms accounting for this metabolic defect remained unresolved. Here, we have examined the role of glucose-6-phosphate dehydrogenase (G6PDH) activity in the pathogenesis of insulin resistance in skeletal muscle.

Methods: Multiple mouse disease states exhibiting insulin resistance and glucose intolerance, as well as obese humans defined as insulin-sensitive, insulin-resistant, or pre-diabetic, were examined.

Results: We identified increased glucose-6-phosphate dehydrogenase (G6PDH) activity as a common intracellular adaptation that occurs in parallel with the induction of insulin resistance in skeletal muscle and is present across animal and human disease states with an underlying pathology of insulin resistance and glucose intolerance. We observed an inverse association between G6PDH activity and nitric oxide synthase (NOS) activity and show that increasing NOS activity via the skeletal muscle specific neuronal (n)NOSμ partially suppresses G6PDH activity in skeletal muscle cells. Furthermore, attenuation of G6PDH activity in skeletal muscle cells via (a) increased nNOSμ/NOS activity, (b) pharmacological G6PDH inhibition, or (c) genetic G6PDH inhibition increases insulin-independent glucose uptake.

Conclusions: We have identified a novel, previously unrecognized role for G6PDH in the regulation of skeletal muscle glucose metabolism.

Keywords Glucose metabolism; Enzyme activity; Insulin sensitivity

1. INTRODUCTION

Skeletal muscle is one of the largest organs in the human body and, quantitatively, the most important tissue involved in maintaining glucose homeostasis under insulin-stimulated conditions [1]. Recently, we demonstrated that skeletal muscle insulin resistance is an early metabolic defect that precedes hyperglycemia and marked weight gain in response to high-fat feeding in mice [2]. While insulin resistance was associated with elevated lipid species we and others have shown a disconnect between these parameters [3,4]. Furthermore, while inflammatory markers have been linked to skeletal muscle insulin resistance [5], gross changes in skeletal muscle inflammation appear to occur well after the induction of insulin resistance [2]. Likewise, in our hands, adipose tissue macrophage accumulation does not affect whole-body insulin action [6]. Thus, other cellular perturbations likely contribute to skeletal muscle insulin resistance.

Another cause of skeletal muscle insulin resistance could be an altered cellular redox state. In cells, the pyridine nucleotide NADPH is required for a number of processes, including maintenance of the cellular redox balance and antioxidant defense [7]. NADPH is required for the

[1]Cellular and Molecular Metabolism Laboratory, Baker IDI Heart & Diabetes Institute, Melbourne, VIC, Australia [2]Muscle Research and Therapeutics Laboratory, Baker IDI Heart & Diabetes Institute, Melbourne, VIC, Australia [3]Metabolic and Vascular Physiology Laboratory, Baker IDI Heart & Diabetes Institute, Melbourne, VIC, Australia [4]Diabetes & Metabolism Division, Garvan Institute of Medical Research, NSW, Australia [5]Basic and Clinical Myology Laboratory, Department of Physiology, The University of Melbourne, Melbourne, VIC, Australia [6]Institute for Sports, Exercise and Active Living, Victoria University, Footscray, VIC, Australia [7]School of Exercise and Nutrition Sciences, Deakin University, Burwood, VIC, Australia [8]Vascular Biology and Immunopharmacology Group, Department of Pharmacology, Monash University, Clayton, VIC, Australia

[9] Current address: Centre for Exercise and Nutrition, Mary MacKillop Institute for Health Research, Australian Catholic University, Melbourne, VIC, Australia.

[10] Current address: School of Biosciences, The University of Melbourne, Melbourne, VIC, Australia.

*Corresponding author. Mouse Metabolic Phenotyping Facility, Metabolic Disease and Obesity Program, Biomedicine Discovery Institute, Monash University, Clayton, VIC, 3800, Australia. E-mail: robert.lee-young@monash.edu (R.S. Lee-Young).

**Corresponding author. Division of Diabetes & Metabolism, Garvan Institute of Medical Research, 384 Victoria St, Darlinghurst, NSW, 2010, Australia. E-mail: m.febbraio@garvan.org.au (M.A. Febbraio).

Received July 29, 2016 • Revision received August 29, 2016 • Accepted September 5, 2016 • Available online 9 September 2016

http://dx.doi.org/10.1016/j.molmet.2016.09.002

conversion of oxidized to reduced glutathione (GSSG and GSH, respectively), the primary redox buffer of the cell, which has been shown to be dysregulated in insulin resistant skeletal muscle of rodents and humans [8]. Thus, ensuring adequate cellular NADPH levels is a key requirement for cellular homeostasis. Nevertheless, insulin resistance could also be a by-product of maintaining cellular NADPH levels. Indeed, NAPDH is also the major substrate for NADPH oxidase (Nox), a membrane bound enzyme complex, which generates superoxide ($O_2^{\bullet -}$). Excess $O_2^{\bullet -}$ production has been linked to insulin resistance in skeletal muscle via peroxynitrite ($ONOO^{\bullet -}$) formation [9], and in skeletal muscle the time course of increased Nox expression closely parallels the induction of insulin resistance in response to high-fat feeding [10,11].

In skeletal muscle cells, maintenance of NADPH relies heavily on glucose-6-phosphate dehydrogenase (G6PDH) [12], an enzyme most commonly associated with the pentose phosphate pathway [13]. G6PDH is activated in response to extracellular oxidants that cause a decrease in NADPH levels [14]. Under *in vitro* conditions, it can be regulated by NADPH:$NADP^+$ levels [15]. In diet- and genetic-induced animal models of insulin resistance, G6PDH activity is elevated in adipose tissue [16]. In humans, adipose tissue G6PDH mRNA levels are positively associated with BMI [16], while adenoviral overexpression of G6PDH causes insulin resistance in 3T3-L1 adipocyte cells [16]. Whether G6PDH is mechanistically linked to insulin action in skeletal muscle is unclear.

A potential mechanism linking an altered cellular redox state to insulin resistance is nitric oxide synthase (NOS). In skeletal muscle, the generation of nitric oxide (NO) is regulated by the skeletal muscle specific neuronal NOS isozyme (nNOSμ), which is impaired in insulin resistant states of rodents and humans [17–19]. Similarly, nNOSμ protein expression is almost absent in animal models of muscular dystrophy, and, through the use of this model, it was shown that NO was required to repress G6PDH expression and activity [20]. Thus, it is possible that reduced nNOSμ expression in skeletal muscle of insulin resistant states leads to elevated G6PDH. Alternatively, an increase in $O_2^{\bullet -}$ production – arising from increased Nox – could utilize NO to form $ONOO^{\bullet -}$, which would also act to reduce available NO and lead to increased G6PDH. Collectively, these findings suggest that an altered redox state and/or changes in NO availability (via altered expression of nNOSμ) could be contributing to the onset of skeletal muscle insulin resistance. Thus, we examined whether changes in intramuscular redox state contribute to the induction of insulin resistance in skeletal muscle.

2. MATERIAL AND METHODS

2.1. Animals

C57Bl/6 mice used for the chow-fed and HFD studies have been previously described [2]. C57Bl/10 and *mdx* mice as well as *ob*/+ and *ob*/*ob* littermates were bred in-house (AMREP Animal Services, Melbourne, VIC, Australia). For PBS and C-26 experiments, 21 wk old CD2F1 mice were used as previously described [21]. *nnos*$^{+/+}$ and *nnos*$^{+/-}$ littermate mice were generated by breeding C57Bl/6 nNOS$^{+/-}$ mice originally obtained from Jackson Laboratories (Bar Harbor, ME). All mice were maintained at 22 ± 1 °C on a 12:12 h light–dark cycle with free access to food and water. All procedures undertaken were approved by the AMREP Animal Ethics Committee or the Animal Ethics Committee of The University of Melbourne, and conducted in accordance with the Australian code of practice for the care and use of animals for scientific purposes as stipulated by the National Health and Medical Research Council of Australia.

2.2. Human experiments

Muscle biopsies were collected after an overnight fast from obese insulin sensitive (IS), obese insulin resistant (IT), and pre-diabetic individuals. All protocols were approved by either the Alfred Hospital Human Research Ethics Committee (Melbourne, VIC, Australia) or St. Vincent's Hospital Human Research Ethics Committee (Sydney, NSW, Australia) and conducted in accordance with the Declaration of Helsinki of the World Medical Association. All volunteers provided written informed consent.

2.3. Adenovirus production

Human nNOSμ cDNA was synthesized by GenScript (Piscataway, NJ, USA). Recombinant adenovirus was produced by transfecting HEK293T cells grown to 80–90% confluency. The adenovirus was purified using Mustang QTM ion exchange discs (Pall Corporation, NY, USA) according to manufacturer's instructions. Eluted virus was then concentrated and stored at −80 °C.

2.4. Cell culture experiments

Cell culture experiments were performed on L6 myotubes free of mycoplasma contamination (CRL-1458, ATCC®, USA). For AdV experiments, myotubes were infected with GFP or hu-nNOSμ AdV for 72 h. Glucose transport experiments were performed between passages 2–10 as described [22] using 2-[^{3}H]DG (Perkin Elmer). To determine the effect of G6PDH inhibition on GLUT4 translocation, GLUT4 translocation assays were performed as described on L6 myotubes infected with a retrovirus containing an exofacial HA epitope-tagged construct of human GLUT4 [23]. Stable L6 cells expressing full or partial knockdown of *g6pdh* were generated using a G6PDH shRNA lentivirus in parallel with a scrambled shRNA lentivirus according to the manufacturer's instructions (Santa Cruz Biotechnology Inc.). Where indicated, 6-AN was reconstituted in DMSO (Sigma), and DMSO alone was used as the corresponding control.

2.5. Enzymatic assays

G6PDH activity was measured as the difference between 6-phosphogluconate dehydrogenase (6-PG) activity and total dehydrogenase activity (G6PDH + 6-PG). Samples (~10–20 μg) were incubated in assay buffer (0.1 M Tris–HCl, 500 μM EDTA, 500 μM NADP) with 200 μM 6-phosphogluconate (6-PG activity) or 200 μM G6P + 200 μM 6-phosphogluconate (total activity), and the rate of NADPH production at 340 nm was determined over 20 min (FLUOstar Omega, Life Technologies).

Pyridine nucleotide levels were determined on acid or alkali extracted samples as described [24]. Briefly, ~10–20 μg of protein was added to alkali buffer (0.05 M NaOH, 1 mM EDTA) and then divided into two aliquots. In one of the aliquots, an equal volume of 0.1 M HCl was added to generate an acid extract, and both extracts were then heated at 60 °C for 30 min. The alkali extract was neutralized with 100 mM Tris–HCl (pH 8.1) and 0.05 M HCl. The acid extract was neutralized with 0.4 M Tris. $NADP^+$ and NADPH were measured essentially as described [25] with the exception being that glutamate dehydrogenase and G6PDH, respectively, were used as substrates. The rate of change was measured over 30 min.

NOS activity was determined as described [26] as was GPx activity [27]. GSH(t) and GSSG levels were determined using enzymatic recycling [28]. NADK activity was determined as described and calculated as the difference between samples incubated with and without NAD^+ and ATP.

2.6. RNA isolation and quantitative real-time RT-PCR

Total RNA was isolated from skeletal muscle tissue using Trizol (Invitrogen, Carlsbad, CA). Samples were reverse transcribed using

Taqman reverse transcription reagents (Applied Biosystems, Foster City, CA, USA). Gene expression analysis was performed by RT-PCR using TaqMan gene expression assays (Applied Biosystems), including 18S probe and primers for housekeeping measurements.

2.7. Statistics

Data are expressed as mean ± standard deviation of the mean (SD). Data were analyzed by t-test, one-way analysis of variance (ANOVA), two-way ANOVA, two-way repeated measures ANOVA, or linear regression where appropriate using SigmaPlot (version 10.0, Systat Software Inc.). Where significance was $p < 0.05$, Fisher's least significance difference test was used to determine differences between groups.

3. RESULTS

3.1. Altered redox state and induction of insulin resistance in skeletal muscle are temporally related

Previously, we demonstrated the induction of skeletal muscle insulin resistance following 3 wk of a high-fat diet (HFD) in mice [2]. After 3 wk of a HFD in mice, we observed a trend ($p = 0.09$) for reduced NADPH levels and increased $NADP^+$ under 5 h fasted conditions (Figure 1A), leading to a reduction in the NADPH:$NADP^+$ ratio within *gastrocnemius* muscle (Figure 1B). Increased $NADP^+$ levels were not due to elevated NAD^+ kinase activity (Figure S1A). Likewise, total GSH levels were unchanged (Figure S1B), while GSSG levels were reduced by ~20% (Figure S1C). There was no difference in the GSH:GSSG ratio (Figure S1D). The activity of glutathione peroxidase, responsible for reducing H_2O_2 to H_2O, was also unaltered (Figure S1E).

In contrast, mRNA levels of Nox2 and Nox4, as well as the regulatory $p47^{phox}$ subunit were increased by 30–50% after 3 wk of the HFD (Figure 1C), whereas tyrosine nitration — an indicator of $ONOO^{\bullet-}$ formation — was unaltered (Figure S1F). The activity of G6PDH was also elevated in 3 wk HFD mice (Figure 1D). This phenomenon was not isolated to specific muscle groups, as we observed a similar finding in superficial *vastus lateralis* of mice fed a HFD for 3 wk (Figure S2A). However, elevated G6PDH activity was not due to differences in *g6pdh* gene expression (Figure S2B). In *gastrocnemius* muscle, we saw a progressive increase in basal G6PDH activity from 3 to 16 wk of a HFD (Figure 1D) and observed a correlation between skeletal muscle G6PDH activity and fat mass in mice (Figure S2C). Furthermore, we saw a trend ($p = 0.08$) for an inverse relationship between skeletal muscle G6PDH activity and basal rates of whole-body glucose disposal (R_d) across the 16 wk HFD period (Figure 1E), and an association between skeletal muscle G6PDH activity and basal rates of hepatic glucose production (Figure S2D).

It has previously been shown that both G6PDH expression and activity is elevated in adipose tissue of dietary and genetically obese animal models [16]. Given that the 3 wk HFD mice were glucose intolerant (Figure 2A), we next assessed G6PDH activity and found it to be elevated by ~45% under fasted conditions in skeletal muscle of *ob/ob* mice, which are also glucose intolerant (Figure 2B), when compared with *ob*/+ littermates (Figure 2C). Likewise, G6PDH activity was elevated in *mdx* mice (Figure S3A), which share the same X-linked pattern of inheritance to human Duchenne muscular dystrophy and are glucose intolerant [29], under fasted conditions, as well as the pre-clinical colon-26 (C-26) cancer cachexia mouse model, which also exhibits glucose intolerance (Figure S3B and C).

3.2. Skeletal muscle G6PDH activity is linked to NO bioavailability

There is evidence to suggest that NO production, and thus nNOSμ, plays a key role in the regulation of G6PDH in skeletal muscle [20]. To determine whether a relationship exists between nNOSμ expression/NOS activity and G6PDH, we examined $nnos^{+/-}$ mice which have a ~50% reduction in skeletal muscle NOS activity compared with littermate ($nnos^{+/+}$) mice (Figure 3A). As shown in Figure 3B, under fasted conditions, skeletal muscle G6PDH activity was elevated by ~45% in $nnos^{+/-}$ mice. We next assessed NOS activity in our animal models with elevated G6PDH activity. Despite unaltered nNOSμ protein expression in response to a 3 wk HFD (0.33 ± 0.20 vs. 0.25 ± 0.04

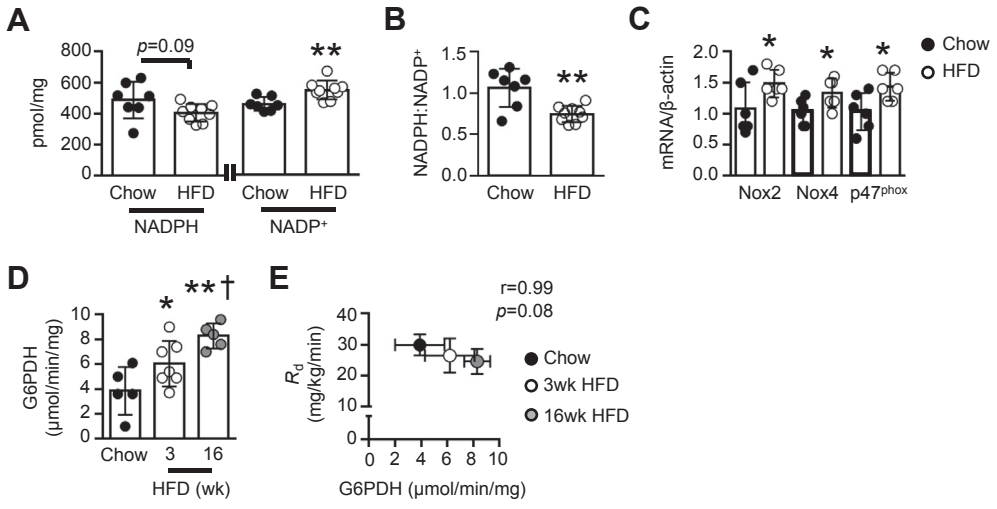

Figure 1: Effect of a high-fat diet (HFD) on skeletal muscle redox state *in vivo*. (A) NADPH and $NADP^+$ levels and (B) NADPH:$NADP^+$ in *gastrocnemius* muscle of chow-fed and 3 wk HFD mice ($n = 7–9$). (C) Nox2, Nox4 and $p47^{phox}$ mRNA expression in *gastrocnemius* muscle of chow-fed and 3 wk HFD mice, normalized to β-actin ($n = 6$). (D) Basal G6PDH activity in *gastrocnemius* muscle of chow-fed, 3 wk HFD, and 16 wk HFD mice ($n = 5–7$). (E) Correlation between mean basal G6PDH activity in *gastrocnemius* muscle of chow-fed ($n = 5$), 3 wk HFD ($n = 7$), and 16 wk HFD mice ($n = 5$) and whole-body glucose disposal (R_d; $n = 10$, 6, and 5, respectively). Data are presented as a scatter plot (bar denotes mean ± S.D; A–D) or mean ± S.D (E), and were analyzed using a two-tailed unpaired t-test (A–C), one-way ANOVA (D), or linear regression analysis (E). *$p < 0.05$, **$p < 0.01$ vs. corresponding Chow group; †$p < 0.05$ vs. 3 wk HFD group.

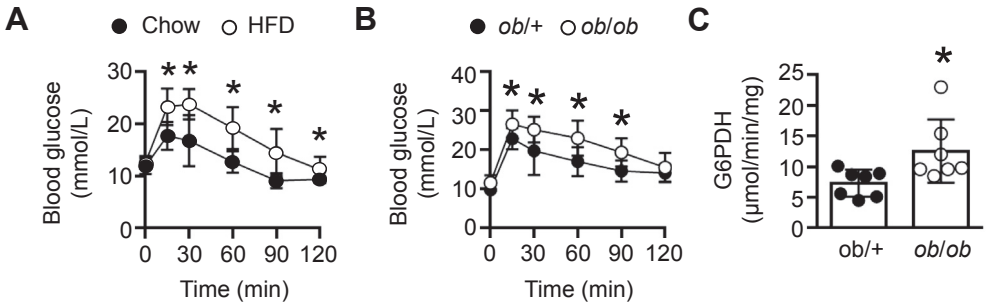

Figure 2: Skeletal muscle G6PDH activity in glucose intolerant animal models. (A) Blood glucose levels in chow-fed and 3 wk HFD mice in response to a glucose tolerance test ($n = 12-19$). (B) Blood glucose levels in *ob*/+ and *ob*/*ob* mice in response to a glucose tolerance test ($n = 7-10$). (C) G6PDH activity in *gastrocnemius* muscle of *ob*/+ and *ob*/*ob* mice ($n = 7$). Data are presented as mean ± S.D (A, B), or scatter plot (bar denotes mean ± S.D; C) and were analyzed using a two-way repeated measures ANOVA (A, B) or a two-tailed unpaired t-test (C). *$p < 0.05$.

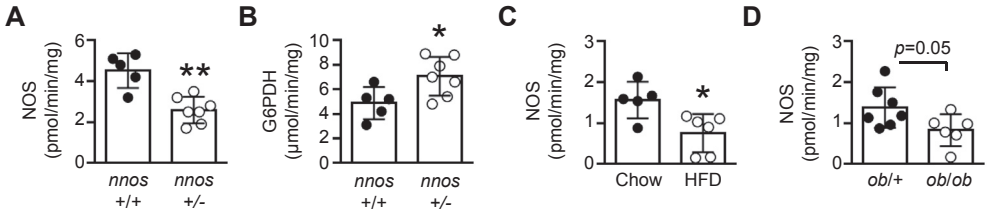

Figure 3: Skeletal muscle G6PDH activity is related to nitric oxide bioavailability. (A) *Gastrocnemius* muscle NOS activity, and (B) G6PDH activity in *nnos*$^{+/+}$ and *nnos*$^{+/-}$ mice ($n = 5-7$). *Gastrocnemius* muscle NOS activity in (C) chow-fed and 3 wk HFD mice ($n = 5-6$), and (D) *ob*/+ and *ob*/*ob* littermates ($n = 7$). Data are presented as a scatter plot (bar denotes mean ± S.D) and were analyzed using a two-tailed unpaired t-test (A–D). *$p < 0.05$, **$p < 0.01$ vs. corresponding control group.

arbitrary units for Chow; $p = 0.4$ for $n = 5$ per group), NOS activity was reduced in skeletal muscle (Figure 3C). There was also a trend ($p = 0.05$) for reduced NOS activity in skeletal muscle of *ob*/*ob* mice (Figure 3D), while NOS activity was almost absent in skeletal muscle of *mdx* mice (Figure S3D). In contrast, no differences in NOS activity were observed in skeletal muscle of PBS and C-26 injected mice (Figure S3E). Linear regression analysis revealed that G6PDH activity was inversely correlated to NOS activity in skeletal muscle *in vivo* across all animal models, including the C-26 cancer cachexia model (Figure S3F).

3.3. Skeletal muscle G6PDH activity is regulated by NO bioavailability

In non-muscle tissue, hyperglycemia and palmitate have been shown to decrease G6PDH activity, whereas insulin has been shown to increase it [30–32]. We have previously shown that both intramuscular lipids and plasma insulin levels are elevated in mice after 3 wk of a HFD [2]. However, incubation of L6 myotubes with 100 nM insulin for 24 h, 25 mM glucose for 24 h, or 750 µM palmitate for 16 h did not alter G6PDH activity (data not shown). Thus, we focused on the role of nNOSµ in the regulation of G6PDH activity.

To confirm a direct relationship between G6PDH and nNOSµ bioavailability in skeletal muscle, we utilized L6 myotubes, which have undetectable levels of endogenous NOS expression (see nNOSµ expression and NOS activity in GFP treated cells; Figure S4A and B, respectively). We infected L6 myotubes (see Figure S4C for representative GFP adenovirus infection) with two different doses of a human nNOSµ (hu-nNOSµ) adenovirus. Infection with six infectious units (6IU) resulted in a small increase in nNOSµ protein expression but no change in NOS activity. Infection with 14IU increased nNOSµ protein expression and NOS activity (Figure S4A and B, respectively). Compared with GFP, hu-nNOSµ at 6IU did not alter G6PDH activity (Figure S4D). Overexpression of hu-nNOSµ at 14IU suppressed G6PDH activity by ~35% (Figure 4A), indicating that nNOSµ plays a direct role in regulating G6PDH in skeletal muscle.

3.4. Partial suppression of G6PDH activity enhances insulin-independent glucose uptake in skeletal muscle

When hu-nNOSµ was expressed at 6IU in L6 myotubes, we saw no alteration in 2-[^{3}H]deoxyglucose (2-[^{3}H]DG) uptake under basal (i.e. insulin-dependent) or insulin-stimulated conditions when compared with GFP treated cells (Figure S4E). However, hu-nNOSµ at 14IU increased basal rates of 2-[^{3}H]DG uptake, resulting in enhanced rates of 2-[^{3}H]DG uptake under insulin-stimulated conditions (Figure 4B, left panel). Indeed, no differences were observed in insulin-stimulated 2-[^{3}H]DG uptake *per se* in response to hu-nNOSµ at 14IU (Figure 4B, right panel), indicating that the elevated rates of insulin-stimulated 2-[^{3}H]DG uptake was due to enhanced basal 2-[^{3}H]DG uptake. In ZDF skeletal muscle *in vivo* and also skeletal muscle cell culture, overexpression of nNOSα (lacking the 34 amino acid insert present in nNOSµ [33]) increases GLUT4 protein expression. However, in L6 myotubes hu-nNOSµ at 6IU or 14IU did not alter total GLUT4 levels (Figure S5A). Similarly, hu-nNOSµ at 14IU did not alter GLUT4 in the membrane fraction under basal or insulin-stimulated conditions (Figure 4C).

To determine whether G6PDH *per se* was involved in the regulation of glucose uptake in skeletal muscle, we induced partial suppression of G6PDH in L6 myotubes via a 24 h incubation with 100 µM of the selective G6PDH inhibitor, 6-aminonicotinamide (6-AN). 6-AN suppressed G6PDH activity by ~15% (Figure 4D), and, as we observed

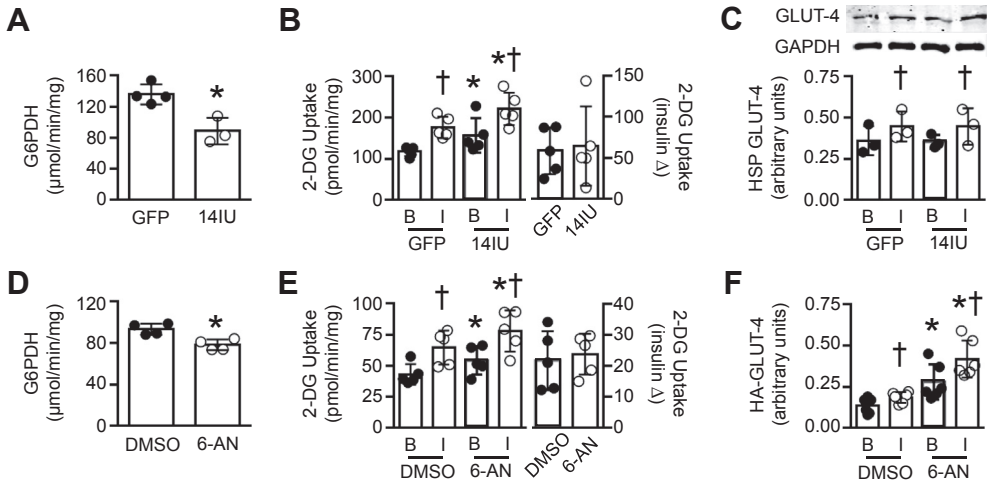

Figure 4: Effect of G6PDH suppression on glucose uptake in L6 myotubes. (A) G6PDH activity following a 72 h adenoviral infection with GFP or 14IU hu-nNOSμ ($n = 3$–4, 3 replicates per experiment). (B) Basal [B] and insulin-stimulated [I] rates of 2-[^{3}H]deoxyglucose (2-[^{3}H]DG) uptake and insulin-stimulated increase in 2-[^{3}H]DG in L6 myotubes following GFP or 14IU hu-nNOSμ infection ($n = 5$, 3–5 replicates per experiment). (C) GLUT-4 protein levels in the high speed pellet fraction (HSP) under basal [B] and insulin-stimulated [I] conditions following a 72 h adenoviral infection with GFP or 14IU hu-nNOSμ ($n = 3$). (D) G6PDH activity in L6 myotubes incubated for 24 h with DMSO or 100 μM 6-AN ($n = 4$, 3 replicates per experiment). (E) Basal [B] and insulin-stimulated [I] rates of 2-[^{3}H]DG uptake and insulin-stimulated increase in 2-[^{3}H]DG following a 24 h incubation with DMSO or 100 μM 6-AN ($n = 5$, 3–5 replicates per experiment). (F) Membrane bound GLUT-4 protein levels under basal [B] and insulin-stimulated [I] conditions following a 24 h incubation with DMSO or 100 μM 6-AN ($n = 6$). Data are presented as a scatter plot (bar denotes mean ± S.D) and were analyzed using a two-tailed unpaired t-test (A, D) or two-way ANOVA (B, C, E, F). *$p < 0.05$ vs. GFP or 6-AN; †$p < 0.05$ vs. corresponding basal group.

with our hu-nNOSμ experiments, 6-AN significantly increased basal rates of 2-[^{3}H]DG uptake, leading to higher rates of insulin-stimulated glucose transport (Figure 4E, left panel). As with hu-nNOSμ, no differences were observed in insulin-stimulated 2-[^{3}H]DG uptake *per se* in response to 6-AN (Figure 4E, right panel). 6-AN did not alter total GLUT4 levels (Figure S5B), but did increase the amount of HA-tagged GLUT4 at the surface of L6 myotubes under basal and insulin-stimulated conditions (Figure 4F).

We also generated stable L6 cell lines expressing (a) endogenous G6PDH activity (termed WT), (b) a partial reduction in G6PDH activity (m8), or (c) whole knockdown of G6PDH activity (m10). Despite achieving full G6PDH knockdown in m10 cells (Figure S5C), these cells had a reduction in basal 2-[^{3}H]DG uptake and did not respond to insulin (Figure S5D). No differences were observed between WT and m8 myotubes, which had a ~45% reduction in G6PDH activity (Figure 5A). However, basal rates of 2-[^{3}H]DG uptake were elevated in m8 cells, again leading to elevated rates of insulin-stimulated 2-[^{3}H]DG uptake (Figure 5B, left panel). Moreover, in m8 cells the insulin-stimulated increase in 2-[^{3}H]DG uptake was increased (Figure 5B, right panel).

3.5. G6PDH activity is increased in skeletal muscle of pre-diabetic individuals

We next determined whether skeletal muscle G6PDH activity was altered in humans with metabolic disease. Specifically, we examined a cohort of glucose tolerant obese individuals who had previously been characterized as exhibiting muscle IS or muscle IR [34], and a cohort of obese individuals who were glucose intolerant and classified as pre-diabetic (fasting blood glucose levels ranging from 5.6 to 6.9 mmol/L and/or blood glucose levels of 7.8–11.0 mmol/L 2 h following an oral glucose tolerance test; HbA1c of 5.7–6.4%; [35]). Participants were matched for age and BMI (Table 1).

While there was no difference in basal skeletal muscle G6PDH activity in IS and IR groups, G6PDH activity was elevated in pre-diabetic individuals (Figure 6A). In humans, adipose tissue G6PDH is positively associated with BMI [16], although we did not observe this association with regard to skeletal muscle G6PDH activity (Figure S6A). When examining our data from patients with pre-diabetes, while all individuals exhibited 2 h OGTT glucose levels of 7.8–10.9 mmol/L, 13 individuals had normal fasting glucose levels (range of 4.4–5.5 mmol/

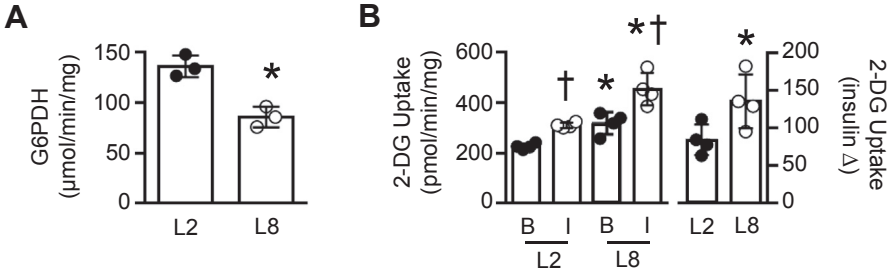

Figure 5: Genetic reduction of G6PDH activity increases insulin-independent glucose transport. (A) G6PDH activity in stable L6 myotubes infected with scrambled (L2) or *g6pd* shRNA (L8) ($n = 3$, 3 replicates per experiment). (B) Basal [B] and insulin-stimulated [I] rates of 2-[^{3}H]deoxyglucose (2-[^{3}H]DG) transport, and insulin-stimulated increase in 2-[^{3}H]DG in stable L6 myotubes infected with scrambled (L2) or *g6pd* shRNA (L8) ($n = 4$, 3–4 replicates per experiment). Data are presented as a scatter plot (bar denotes mean ± S.D) and were analyzed using a two-tailed unpaired t-test (A), or a two-way ANOVA (B). †$p < 0.05$ vs. Corresponding L2; *$p < 0.05$ vs. corresponding basal.

Table 1 — Characteristics of obese insulin sensitive, obese insulin resistant, and obese pre-diabetic subjects.

Parameter	Insulin sensitive ($n = 16$)	Insulin resistant ($n = 24$)	Pre-diabetic ($n = 24$)
Gender (M:F)	6:10	14:10	19:5
Age (years)	51 ± 14	48 ± 10	55 ± 8
BMI (kg/m^2)	36 ± 4	36 ± 4	34 ± 6
Fasting glucose (mmol/L)	4.7 ± 0.4	4.9 ± 0.4	5.4 ± 0.6**
Fasting insulin (pmol/L)	85 ± 37	171 ± 104††	107 ± 62
2 h OGTT glucose (mmol/L)	5.4 ± 1.4	5.8 ± 1.2	9.1 ± 1.0**
HbA1c (%)	5.2 ± 0.2	5.5 ± 0.3†	5.7 ± 0.4**
Plasma triacylglycerol (mmol/L)	0.8 ± 0.3	1.1 ± 0.4	1.5 ± 0.7**

Data are mean ± S.D. and were analyzed using a one-way ANOVA. **$p < 0.001$ vs. insulin sensitive and insulin resistant groups; †$p < 0.05$ vs. insulin sensitive group; ††$p < 0.01$ vs. insulin sensitive and pre-diabetic group.

L), whereas 11 individuals exhibited impaired fasting glucose levels (5.7—6.4 mmol/L). Given the association between muscle G6PDH and basal glucose homeostasis seen in mice, we stratified the pre-diabetic individuals based on normal fasting glucose (NFG) or impaired fasting glucose (IFG) levels (see Figure S6B). When stratified based on fasting glucose levels, skeletal muscle G6PDH activity was similar between IS, IR, and pre-diabetic NFG, but elevated in pre-diabetic IFG (Figure 6B). In line with this finding, we also observed a positive association between basal skeletal muscle G6PDH activity and fasting plasma glucose (Figure 6C), basal skeletal muscle G6PDH activity and fasting plasma glucose:fasting plasma insulin levels (Figure 6D) as well as basal skeletal muscle G6PDH activity and blood glucose levels 2 h following an oral glucose tolerance test (Figure 6E) across all individuals.

3.6. Insulin-stimulated G6PDH activity is defective in insulin resistant skeletal muscle

We have previously shown that insulin sensitivity is reduced in mice following a 3 wk HFD [2]. Accordingly, we next examined whether insulin-stimulated G6PDH activity was also altered. In chow-fed mice, a 2 h hyperinsulinemic-euglycemic clamp (insulin clamp; see [2] for relevant data) increased G6PDH activity 1.8 ± 0.1-fold in *gastrocnemius* muscle, whereas the 3 wk HFD completely suppressed the insulin-stimulated increase in G6PDH activity (0.9 ± 0.1-fold change vs. basal; Figure 7A). Moreover, the insulin-stimulated change in *gastrocnemius* G6PDH activity of chow-fed and 3 wk HFD mice was positively associated with the glucose infusion rate required to maintain euglycemia during the insulin clamp (GIR; Figure 7B), as well as the insulin-stimulated glucose disposal rate (IS-GDR; Figure 7C). We also found similar findings in *superficial vastus lateralis* muscle with regards to insulin-stimulated G6PDH activity (Figure 7D) and the association between G6PDH activity with GIR (Figure 7E) and IS-GDR (Figure 7F).

4. DISCUSSION

Impaired glucose uptake and metabolism within skeletal muscle is a defect seen not only in T2D but also across multiple non-diabetic disease states [36]. We have identified elevated G6PDH activity as a common intramuscular perturbation seen across multiple disease states in animals and humans, all with an underlying pathology of glucose intolerance. We also identified a direct relationship between nNOSμ/NOS activity and the regulation of G6PDH activity in skeletal muscle cells. Moreover, we showed that partial suppression of G6PDH activity via three independent mechanisms (increased nNOSμ/NOS

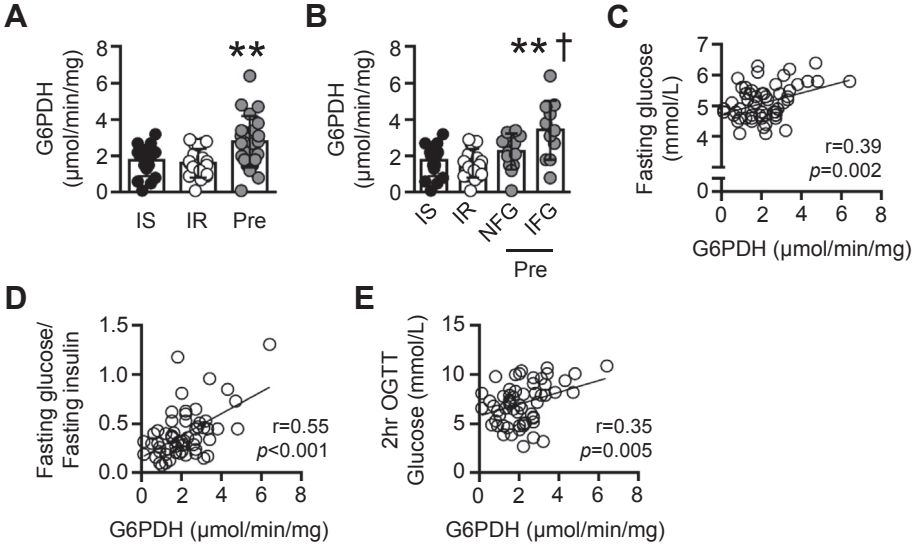

Figure 6: Skeletal muscle G6PDH activity is altered in pre-diabetic individuals. (A) G6PDH activity in *vastus lateralis* muscle of obese insulin sensitive (IS; $n = 17$), obese insulin resistant (IR; $n = 21$), and obese pre-diabetic individuals (Pre; $n = 24$). (B) G6PDH activity in *vastus lateralis* muscle of IS ($n = 17$), IR ($n = 21$), and Pre (stratified for normal fasting glucose (NFG; $n = 13$) and impaired fasting glucose (IFG; $n = 11$) levels). (C) Correlation between basal *vastus lateralis* muscle G6PDH activity and fasting blood glucose levels in IS, IR, and Pre ($n = 62$). (D) Correlation between basal *vastus lateralis* muscle G6PDH activity and fasting glucose:fasting insulin levels in IS, IR, and Pre ($n = 62$). (E) Correlation between basal *vastus lateralis* muscle G6PDH activity and blood glucose levels 2 h following a 75 g oral glucose tolerance test (OGTT) in IS, IR, and Pre ($n = 62$). Data are presented as a scatter plot (bar denotes mean ± S.D) and were analyzed using a one-way ANOVA (A, B), or linear regression analysis (C—E). **$p < 0.01$ vs. IS and IR; †$p < 0.05$ vs. Pre NFG.

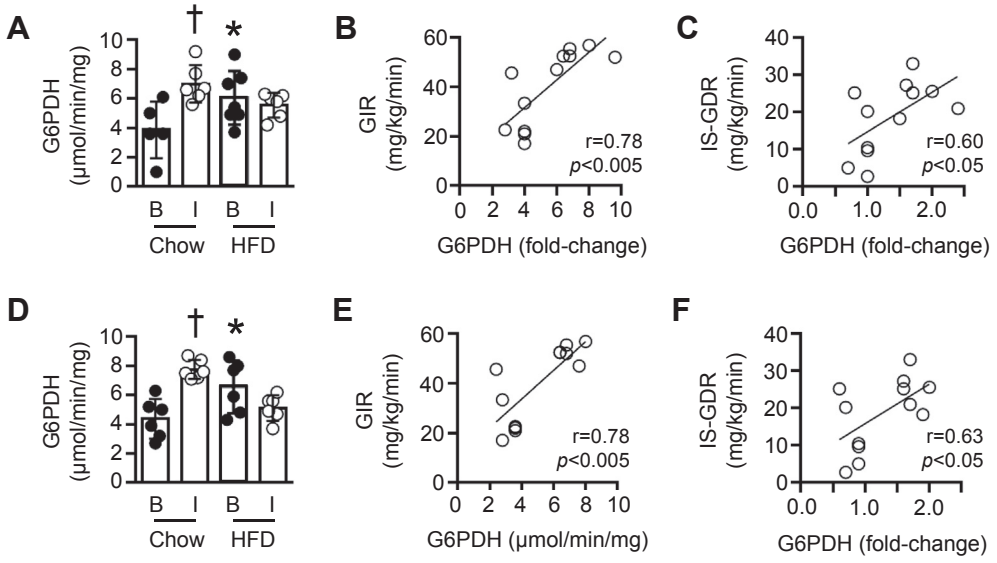

Figure 7: Skeletal muscle G6PDH activity under insulin-stimulated conditions *in vivo*. (A) G6PDH activity in *gastrocnemius* muscle of chow-fed or 3 wk HFD mice under basal conditions [B] or following a 2 h hyperinsulinemic-euglycemic clamp (insulin clamp) [I] ($n = 5–7$). (B) Correlation between the insulin-stimulated increase in *gastrocnemius* G6PDH activity and the glucose infusion rate (GIR) required to maintain euglycemia during the insulin clamp ($n = 12$), or (C) whole-body insulin-stimulated glucose disposal rate (IS-GDR, $n = 12$). (D) G6PDH activity under [B] and [I] conditions ($n = 6$). (B) Correlation between the insulin-stimulated increase in G6PDH activity (expressed as a fold-change vs. corresponding basal group) and GIR during a 2 h hyperinsulinemic-euglycemic clamp ($n = 12$). (C) Correlation between the insulin-stimulated increase in *superficial vastus lateralis* G6PDH activity (expressed as a fold-change vs. corresponding basal group) and the insulin-stimulated glucose disposal rate ($n = 12$). Data are presented as a scatter plot (bar denotes mean ± S.D) and were analyzed using a two-way ANOVA (A, D), or linear regression analysis (B, C, E, F). *$p < 0.05$ vs. corresponding chow group; †$p < 0.01$ vs. corresponding basal value.

activity, pharmacological G6PDH inhibition, and genetic G6PDH inhibition) all acted to increase insulin-independent glucose uptake in skeletal muscle cells. Finally, we identified a defect in skeletal muscle G6PDH activity under insulin-stimulated conditions. Thus, not only do our findings highlight a perturbation in skeletal muscle G6PDH in glucose intolerant states but they also highlight a previously unidentified role for G6PDH in the regulation of skeletal muscle glucose uptake.

Here, we identified a change in the cellular redox state — as evidenced by an altered NADPH:$NADP^+$ ratio — which paralleled the onset of skeletal muscle insulin resistance in response to a HFD in mice. In particular, Nox expression and G6PDH activity were elevated, whereas other markers associated with impaired glucose uptake in response to a HFD were unaltered. This differs from previous findings, which have indicated a predominate role for GSH:GSSG and H_2O_2 production in skeletal muscle insulin resistance in response to high-fat feeding [8]. The reason for these discrepancies is unclear, though they may be related to the specific HFD, which contained significantly more fat in previous studies (~60–100% calories from fat, versus ~40% in the present study). In mice, a prolonged HFD (≥8 wk) increases Nox2, Nox4, and $p47^{phox}$ expression in skeletal muscle [10,11], and here we show a progressive increase in G6PDH activity from 3 to 16 wk of a HFD. Thus, unlike other markers of insulin resistance/glucose intolerance (e.g. inflammation) which only seem to be evident after prolonged high-fat feeding [2], alterations in Nox expression and G6PDH activity are readily detectable in skeletal muscle at a similar time point to that of impaired glucose uptake.

Our findings identify a role for G6PDH in the regulation of insulin-independent glucose uptake *in vivo*. In 3T3-L1 adipocytes, overexpression of G6PDH suppresses insulin-stimulated glucose transport by ~40% [32] in agreement with our current findings in muscle cells whereby partial suppression of G6PDH enhances the rate of glucose transport under insulin-stimulated conditions. However, based on our results, it is clear that the elevated rates of insulin-stimulated glucose transport were due to an additive effect arising from augmented rates of insulin-independent glucose transport. It is possible that G6PDH overexpression in 3T3-L1 adipocytes also altered insulin-independent rates of glucose transport; however, this was not assessed [32]. We observed elevated rates of insulin-independent glucose transport via three independent mechanisms (hu-nNOSμ, 6-AN, *g6pdh* shRNA), all of which partially suppressed G6PDH activity. Given that elevated G6PDH activity was an intracellular defect observed across multiple animal and human glucose intolerant disease states, our findings suggest that targeting G6PDH, or the G6PDH pathway within skeletal muscle, may exert positive effects on glucose homeostasis. However, our finding that cells expressing full knockdown of G6PDH were not functionally viable demonstrates that there is a finite range to which the G6PDH pathway can be modulated.

Our study is the first to specifically examine G6PDH activity in skeletal muscle of humans. Aside from demonstrating that G6PDH is elevated in pre-diabetic individuals, our findings suggest a possible role for endogenous blood glucose levels in the regulation of skeletal muscle G6PDH activity. In this context, it is somewhat surprising that neither high glucose nor high insulin exposure altered G6PDH activity in our L6 skeletal muscle cells. However, this would suggest that (a) glucose or insulin *per se* does not directly regulate G6PDH activity in skeletal muscle, and (b) other factors that are likely absent in L6 muscle cells are required. In this regard, hyperglycemia inhibits endothelial NOS activity in aortic endothelial cells [37]. In a rabbit model of prolonged critical illness, skeletal muscle NOS activity is impaired under normal insulin/hyperglycemia and hyperinsulinemia/hyperglycemia conditions, yet unaltered under hyperinsulinemia/normoglycemia conditions [38]. Given our finding that L6 muscle cells lack endogenous expression of nNOSμ, our data point towards hyperglycemia, through the

manipulation of nNOSμ, as a potential mechanism for the regulation of basal G6PDH activity in skeletal muscle.

A somewhat unexpected finding in the present study was that pharmacological inhibition of G6PDH, via a 24 h incubation with 6-AN, led to increased levels of GLUT4 at the membrane of skeletal muscle cells. The mechanism(s) accounting for this phenomenon is unclear. Furthermore, we did not observe this phenomenon in response to hu-nNOSμ, despite the fact that hu-nNOSμ and 6-AN produced similar results with regards to suppression of G6PDH and increases in insulin-independent glucose uptake. In individuals with T2D, infusion of a NO donor increases basal rates of leg glucose uptake [39]. Studies in isolated muscle strips have shown that this increased glucose uptake occurs through an insulin-independent signaling mechanism(s) [40]. This is consistent with our findings in L6 myotubes showing that changes in glucose uptake in response to hu-nNOSμ occur in the absence of any alteration in GLUT4 levels.

Our findings with regard to insulin-stimulated G6PDH activity are intriguing. Under healthy conditions, we found that insulin increases G6PDH activity in skeletal muscle, yet this increase is ablated after a 3 wk HFD. From a physiological standpoint, one would expect G6PDH activity to increase in response to an acute elevation in insulin, as this increases glucose flux into skeletal muscle and thus elevates G6P. However, the reason that this insulin-stimulated increase in G6PDH activity is not observed following a 3 wk HFD remains unclear. In non-muscle tissue, G6PDH activity can be modulated via phosphorylation, while PI-3 kinase and Akt have been shown to act as positive regulators of G6PDH [13]. We have found no alteration in insulin-stimulated Akt Serine^{473} phosphorylation in skeletal muscle following a 3 wk HFD in mice [2], although it is possible that other regulators of G6PDH are altered in response to the HFD. Thus, it will be important to determine the role of G6PDH in the regulation of insulin-stimulated glucose uptake in skeletal muscle, and the factor(s) that contribute to the increase in G6PDH activity in response to insulin.

5. CONCLUSIONS

In conclusion, we have identified a novel, previously unidentified role for G6PDH in skeletal muscle. Skeletal muscle G6PDH is defective across multiple disease states, in animals and humans, all with an underlying pathology of impaired glucose tolerance. Moreover, G6PDH is directly regulated by nNOSμ/NOS activity, and this interaction appears to play a role in the regulation of insulin-independent glucose uptake. There remains no cure for skeletal muscle insulin resistance. Indeed, while current glucose lowering therapies such as metformin and sulfonylureas indirectly target skeletal muscle to improve glucose uptake [41], their molecular basis is unknown, and efficacy declines over time [42]. The lack of efficacy, combined with adverse complications of current glucose lowering therapies, highlights a clear, clinical unmet need for the treatment of skeletal muscle insulin resistance. Our data suggest that G6PDH may be a novel target by which to increase insulin-independent glucose uptake in skeletal muscle in multiple disease states where glucose intolerance and insulin resistance is manifest.

ACKNOWLEDGEMENTS

We would like to thank Prof. Greg Cooney (University of Sydney, Sydney, NSW, Australia) for constructive comments relating to this manuscript. This work was supported by funding from the National Health and Medical Research Council (NHMRC) of Australia (1004212), the Diabetes Australia Research Trust Program, and the Victorian Government Operational Infrastructure Support Program. RSL, KTM, and PG are supported by career development awards from the NHMRC of Australia. GRD, BAK and MAF are supported by research fellowships from the NHMRC of Australia. All authors declare that there are no conflicts of interest. RSL is the guarantor if this work and, as such, had full access to all the data in the study and takes responsibility for the integrity of the data and the accuracy of the data analysis.

CONFLICT OF INTEREST

None declared.

APPENDIX A. SUPPLEMENTARY DATA

Supplementary data related to this article can be found at http://dx.doi.org/10.1016/j.molmet.2016.09.002.

REFERENCES

[1] DeFronzo, R.A., Ferrannini, E., Sato, Y., Felig, P., Wahren, J., 1981. Synergistic interaction between exercise and insulin on peripheral glucose uptake. The Journal of Clinical Investigation 68:1468–1474.

[2] Turner, N., Kowalski, G.M., Leslie, S.J., Risis, S., Yang, C., Lee-Young, R.S., et al., 2013. Distinct patterns of tissue-specific lipid accumulation during the induction of insulin resistance in mice by high-fat feeding. Diabetologia 56: 1638–1648.

[3] Bosma, M., Kersten, S., Hesselink, M.K., Schrauwen, P., 2012. Re-evaluating lipotoxic triggers in skeletal muscle: relating intramyocellular lipid metabolism to insulin sensitivity. Progress in Lipid Research 51:36–49.

[4] Selathurai, A., Kowalski, G.M., Burch, M.L., Sepulveda, P., Risis, S., Lee-Young, R.S., et al., 2015. The CDP-ethanolamine pathway regulates skeletal muscle diacylglycerol content and mitochondrial biogenesis without altering insulin sensitivity. Cell Metabolism 21:718–730.

[5] Osborn, O., Olefsky, J.M., 2012. The cellular and signaling networks linking the immune system and metabolism in disease. Nature Medicine 18:363–374.

[6] Kraakman, M.J., Kammoun, H.L., Allen, T.L., Deswaerte, V., Henstridge, D.C., Estevez, E., et al., 2015. Blocking IL-6 trans-signaling prevents high-fat diet-induced adipose tissue macrophage recruitment but does not improve insulin resistance. Cell Metabolism 21:403–416.

[7] Ying, W., 2008. NAD+/NADH and NADP+/NADPH in cellular functions and cell death: regulation and biological consequences. Antioxidants & Redox Signaling 10(2):179–206.

[8] Anderson, E.J., Lustig, M.E., Boyle, K.E., Woodlief, T.L., Kane, D.A., Lin, C.T., et al., 2009. Mitochondrial H2O2 emission and cellular redox state link excess fat intake to insulin resistance in both rodents and humans. The Journal of Clinical Investigation 119:573–581.

[9] Hoehn, K.L., Salmon, A.B., Hohnen-Behrens, C., Turner, N., Hoy, A.J., Maghzal, G.J., et al., 2009. Insulin resistance is a cellular antioxidant defense mechanism. Proceedings of the National Academy of Sciences of the United States of America 106:17787–17792.

[10] Furukawa, S., Fujita, T., Shimabukuro, M., Iwaki, M., Yamada, Y., Nakajima, Y., et al., 2004. Increased oxidative stress in obesity and its impact on metabolic syndrome. The Journal of Clinical Investigation 114:1752–1761.

[11] Souto Padron de Figueiredo, A., Salmon, A.B., Bruno, F., Jimenez, F., Martinez, H.G., Halade, G.V., et al., 2015. Nox2 mediates skeletal muscle insulin resistance induced by a high-fat diet. The Journal of Biological Chemistry 290:13427–13439.

[12] Mailloux, R.J., Harper, M.E., 2010. Glucose regulates enzymatic sources of mitochondrial NADPH in skeletal muscle cells; a novel role for glucose-6-phosphate dehydrogenase. FASEB Journal 24:2495–2506.

[13] Stanton, R.C., 2012. Glucose-6-phosphate dehydrogenase, NADPH, and cell survival. IUBMB Life 64:362–369.

[14] Kletzien, R.F., Harris, P.K., Foellmi, L.A., 1994. Glucose-6-phosphate dehydrogenase: a "housekeeping" enzyme subject to tissue-specific regulation by hormones, nutrients, and oxidant stress. FASEB Journal 8:174–181.

[15] Holten, D., Procsal, D., Chang, H.L., 1976. Regulation of pentose phosphate pathway dehydrogenases by NADP+/NADPH ratios. Biochemical and Biophysical Research Communications 68:436–441.

[16] Park, J., Rho, H.K., Kim, K.H., Choe, S.S., Lee, Y.S., Kim, J.B., 2005. Overexpression of glucose-6-phosphate dehydrogenase is associated with lipid dysregulation and insulin resistance in obesity. Molecular and Cellular Biology 25:5146–5157.

[17] Bradley, S.J., Kingwell, B.A., Canny, B.J., McConell, G.K., 2007. Skeletal muscle neuronal nitric oxide synthase micro protein is reduced in people with impaired glucose homeostasis and is not normalized by exercise training. Metabolism 56:1405–1411.

[18] Kashyap, S.R., Roman, L.J., Lamont, J., Masters, B.S., Bajaj, M., Suraamornkul, S., et al., 2005. Insulin resistance is associated with impaired nitric oxide synthase activity in skeletal muscle of type 2 diabetic subjects. The Journal of Clinical Endocrinology and Metabolism 90:1100–1105.

[19] Young, M.E., Leighton, B., 1998. Evidence for altered sensitivity of the nitric oxide/cGMP signalling cascade in insulin-resistant skeletal muscle. The Biochemical Journal 329:73–79.

[20] Cacchiarelli, D., Martone, J., Girardi, E., Cesana, M., Incitti, T., Morlando, M., et al., 2010. MicroRNAs involved in molecular circuitries relevant for the Duchenne muscular dystrophy pathogenesis are controlled by the dystrophin/nNOS pathway. Cell Metabolism 12:341–351.

[21] Murphy, K.T., Struk, A., Malcontenti-Wilson, C., Christophi, C., Lynch, G.S., 2013. Physiological characterization of a mouse model of cachexia in colorectal liver metastases. American Journal of Physiology. Regulatory, Integrative and Comparative Physiology 304:R854–R864.

[22] Hutchinson, D.S., Bengtsson, T., 2005. αA-adrenoceptors activate glucose uptake in L6 muscle cells through a phospholipase C-, phosphatidylinositol-3 kinase-, and atypical protein kinase C-dependent pathway. Endocrinology 146:901–912.

[23] Govers, R., Coster, A.C., James, D.E., 2004. Insulin increases cell surface GLUT4 levels by dose dependently discharging GLUT4 into a cell surface recycling pathway. Molecular and Cellular Biology 24:6456–6466.

[24] Lin, S.S., Manchester, J.K., Gordon, J.I., 2001. Enhanced gluconeogenesis and increased energy storage as hallmarks of aging in Saccharomyces cerevisiae. The Journal of Biological Chemistry 276:36000–36007.

[25] Jacobson, E.L., Jacobson, M.K., 1997. Tissue NAD as a biochemical measure of niacin status in humans. Methods in Enzymology 280:221–230.

[26] Lee-Young, R.S., Ayala, J.E., Hunley, C.F., James, F.D., Bracy, D.P., Kang, L., et al., 2010. Endothelial nitric oxide synthase is central to skeletal muscle metabolic regulation and enzymatic signaling during exercise in vivo. American Journal of Physiology. Regulatory, Integrative and Comparative Physiology 298:R1399–R1408.

[27] de Haan, J.B., Bladier, C., Griffiths, P., Kelner, M., O'Shea, R.D., Cheung, N.S., et al., 1998. Mice with a homozygous null mutation for the most abundant glutathione peroxidase, Gpx1, show increased susceptibility to the oxidative stress-inducing agents paraquat and hydrogen peroxide. The Journal of Biological Chemistry 273:22528–22536.

[28] Rahman, I., Kode, A., Biswas, S.K., 2006. Assay for quantitative determination of glutathione and glutathione disulfide levels using enzymatic recycling method. Nature Protocols 1:3159–3165.

[29] Stapleton, D.I., Lau, X., Flores, M., Trieu, J., Gehrig, S.M., Chee, A., et al., 2014. Dysfunctional muscle and liver glycogen metabolism in mdx dystrophic mice. PLoS One 9:e91514.

[30] Park, J., Choe, S.S., Choi, A.H., Kim, K.H., Yoon, M.J., Suganami, T., et al., 2006. Increase in glucose-6-phosphate dehydrogenase in adipocytes stimulates oxidative stress and inflammatory signals. Diabetes 55:2939–2949.

[31] Zhang, Z., Apse, K., Pang, J., Stanton, R.C., 2000. High glucose inhibits glucose-6-phosphate dehydrogenase via cAMP in aortic endothelial cells. The Journal of Biological Chemistry 275:40042–40047.

[32] Zhang, Z., Liew, C.W., Handy, D.E., Zhang, Y., Leopold, J.A., Hu, J., et al., 2010. High glucose inhibits glucose-6-phosphate dehydrogenase, leading to increased oxidative stress and beta-cell apoptosis. FASEB Journal 24:1497–1505.

[33] Silvagno, F., Xia, H., Bredt, D.S., 1996. Neuronal nitric-oxide synthase-mu, an alternatively spliced isoform expressed in differentiated skeletal muscle. The Journal of Biological Chemistry 271:11204–11208.

[34] Chen, D.L., Liess, C., Poljak, A., Xu, A., Zhang, J., Thoma, C., et al., 2015. Phenotypic characterization of insulin-resistant and insulin-sensitive obesity. The Journal of Clinical Endocrinology and Metabolism 100:4082–4091.

[35] Association AD, 2015. Classification and diagnosis of diabetes. Diabetes Care 38(Supplement 1):S8–S16.

[36] Abdul-Ghani, M.A., DeFronzo, R.A., 2010. Pathogenesis of insulin resistance in skeletal muscle. Journal of Biomedicine & Biotechnology 476279.

[37] Du, X.L., Edelstein, D., Dimmeler, S., Ju, Q., Sui, C., Brownlee, M., 2001. Hyperglycemia inhibits endothelial nitric oxide synthase activity by post-translational modification at the Akt site. The Journal of Clinical Investigation 108:1341–1348.

[38] Ellger, B., Langouche, L., Richir, M., Debaveye, Y., Vanhorebeek, I., Teerlink, T., et al., 2008. Modulation of regional nitric oxide metabolism: blood glucose control or insulin? Intensive Care Medicine 34:1525–1533.

[39] Wang, F., Zhao, Y., Niu, Y., Wang, C., Wang, M., Li, Y., et al., 2012. Activated glucose-6-phosphate dehydrogenase is associated with insulin resistance by upregulating pentose and pentosidine in diet-induced obesity of rats. Hormone and Metabolic Research 44:938–942.

[40] Tiganis, T., 2011. Reactive oxygen species and insulin resistance: the good, the bad and the ugly. Trends in Pharmacological Sciences 32:82–89.

[41] Musi, N., Hirshman, M.F., Nygren, J., Svanfeldt, M., Bavenholm, P., Rooyackers, O., et al., 2002. Metformin increases AMP-activated protein kinase activity in skeletal muscle of subjects with type 2 diabetes. Diabetes 51:2074–2081.

[42] DeFronzo, R.A., Eldor, R., Abdul-Ghani, M., 2013. Pathophysiologic approach to therapy in patients with newly diagnosed type 2 diabetes. Diabetes Care 36(Suppl. 2):S127–S138.

